Clinical Experience with the 0.55T MAGNETOM Free.Star MRI Scanner

Carlos Raúl Sanchez, Lic.[1,2]; Agustín Cano Rivadaneira[1]; Leonardo Herrera[1]; Eduardo García Saiz, M.D.[1]; Claudio Milicchio, M.D.[1]

[1] Department of Diagnostic Imaging, Imágenes MDQ, Mar del Plata, Argentina
[2] Sociedad Latinoamericana de Resonancia Magnética (SOLAREM)

Abstract

We present our clinical experience with the 0.55T MAGNETOM Free.Star MRI scanner in the context of more than three decades of work with 0.5T and 1T systems and with modern 1.5T and 3T systems. We analyze how advances in hardware, AI-based reconstruction algorithms, and new system designs are enabling lower-field MRI to regain a strategic role with competitive diagnostic imaging, reduced susceptibility artifacts, lower operating costs, and greater accessibility. We discuss how a synergy between technology, AI, and human expertise is needed to achieve optimal results.

Introduction

For years, "more Tesla" was considered synonymous with better diagnosis in MRI. However, recent developments show that optimizing the ecosystem, not just the field strength, is redefining clinical practice. This article summarizes my (CR Sanchez) firsthand experience with three 0.5T superconducting MRI systems from 1993 to 2004, with 1T systems in the 1990s, and with 1.5T and 3T systems since 2008, and how this experience informs my evaluation of the 0.55T MAGNETOM Free.Star.



1 A wrist study using the Contour S flexible coil and Deep Resolve Boost. Resolution and acquisition time:
(1A) 0.2 × 0.2 × 3.0 mm, TA 1:30 min,
(1B) 0.2 × 0.2 × 3.0 mm, TA 2:03 min,
(1C) 0.2 × 0.2 × 2.5 mm, TA 2:50 min,
(1D) 0.2 × 0.2 × 2.5 mm, TA 1:38 min.

Key technological improvements in the 0.55T system with AI

The MAGNETOM Free.Star benefits greatly from AI-based image reconstruction: With its Deep Resolve technology, deep neural networks enhance signal, improve contrast, and reduce noise in images acquired with lower native signal-to-noise ratio (SNR), bringing diagnostic quality closer to that of systems with a wider field of view.

Denoising and super-resolution are two further improvements. With supervised and self-supervised learning models applied during the reconstruction stage, the system increases sharpness and preserves critical anatomical details without increasing scan time.

It is also possible to achieve acceleration through learning: By combining parallel acquisition at high field strengths with AI-driven reconstructions, we can reduce scan times while maintaining diagnostic quality — even achieving image quality that was previously impossible on a system with a field strength below one tesla.

The system offers robustness against susceptibility artifacts, with a lower B_0 reducing artifacts in the thoracic, peri-implant, and cranial regions. AI optimizes residual phase correction and distortion compensation.

Outside of AI, the MAGNETOM Free.Star delivers operational efficiency and a simple design: With its DryCool technology, the system requires just 0.7 liters of liquid helium and no refills. It also has fewer structural requirements, a lighter system weight, and lower energy costs. This makes it easier to install in facilities where space is limited and floors cannot be structurally reinforced.

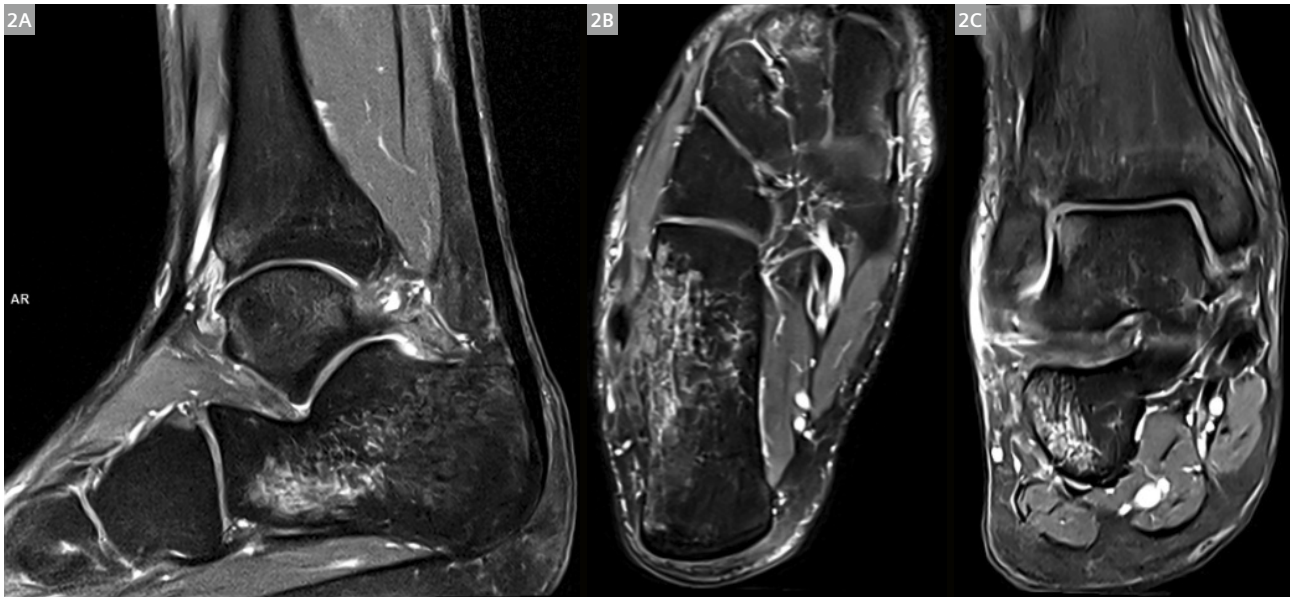
Lower susceptibility is another advantage: Reduced B_0 improves imaging of the chest, peri-implant areas, and cranial regions, producing images with less distortion.

AI also supports automation and workflows with tools for protocol planning, patient positioning, and quality verification. When supervised by experienced MRI technologists, these tools increase reproducibility and performance.

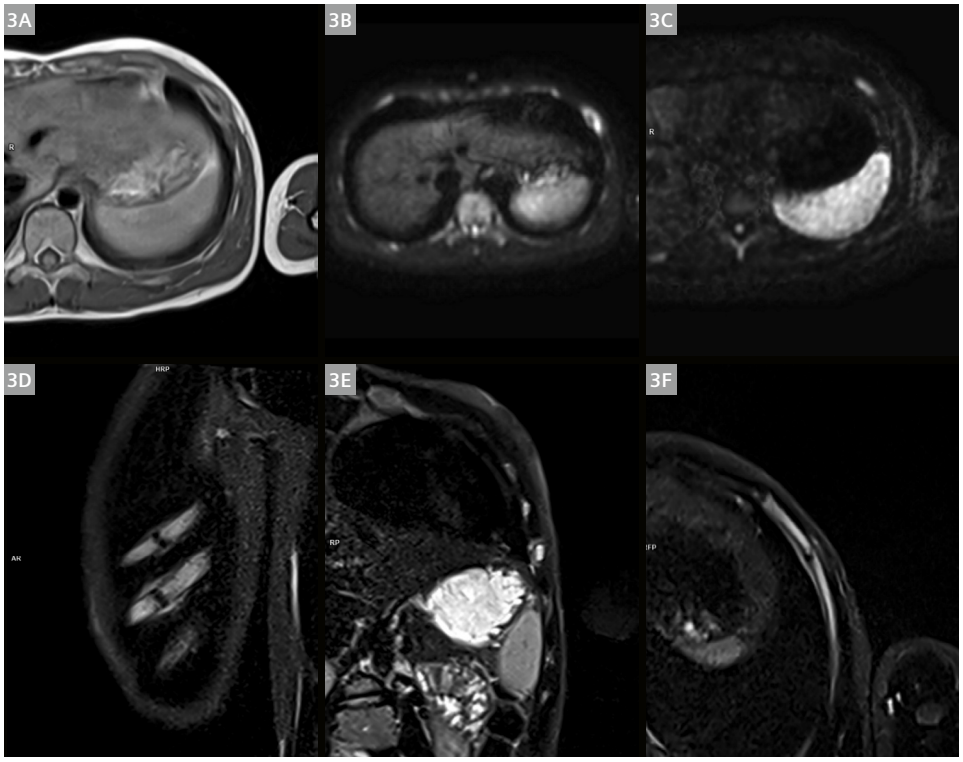
Overall, the MAGNETOM Free.Star combines accessibility, efficiency, reliability, and diagnostic image quality in a single platform. With AI tools such as Deep Resolve reconstruction, the system allows us to achieve excellent results for nearly 90% of the exams that we perform daily on other MRI scanners. As a result, we can deliver more precise patient-centered care and reduce waiting times.

Clinical and practical comparison

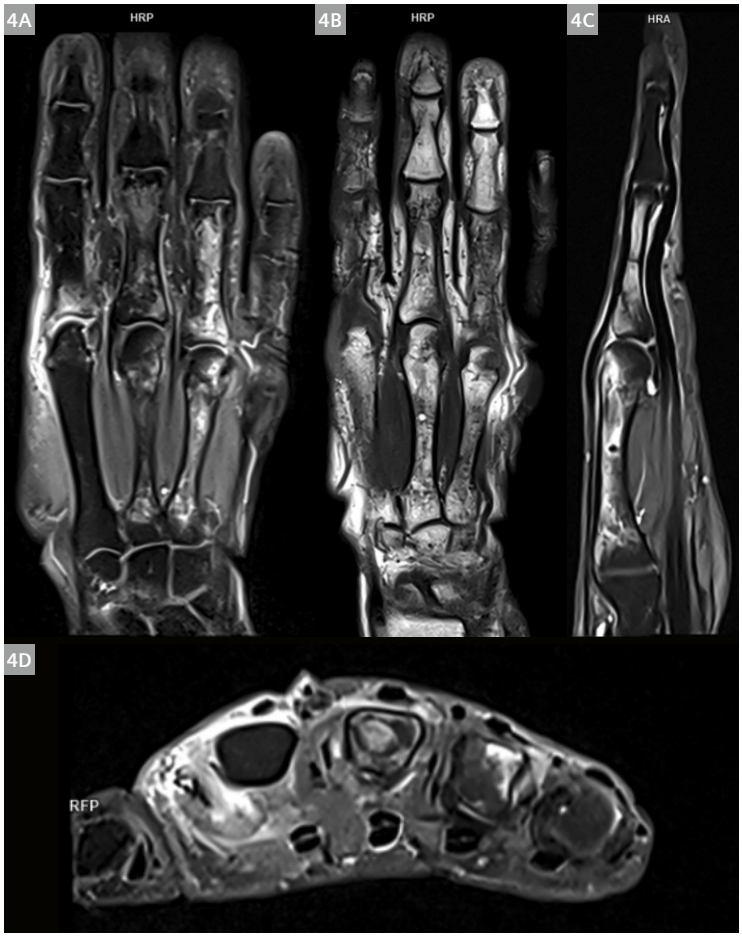
Our operational experience with 0.5T (1993–2004), 1T (since 1994), and 1.5T and 3T (since 2008) MRI scanners gives us a historical perspective that allows us to evaluate the relative advantages and limitations. In what follows, we will share some clinical cases and practical considerations (protocols, TR/TE, FOV) that demonstrate that AI improves results only if the acquisition is technically sound.



2 **(2A)** Heterogeneous hyperintense signal in the posterior and inferior portions of the calcaneus, suggestive of medullary edema/bone hematoma or overload/impaction injury (0.3 × 0.3 × 3.0 mm, TA 1:55 min). **(2B)** Extensive heterogeneous signal increase on T2/STIR in the posterior and plantar portions of the calcaneus, with a multilobulated trabecular pattern occupying a large portion of the posterior calcaneal body (0.3 × 0.3 × 3.0 mm, TA 2:40 min). **(2C)** Area of heterogeneous hyperintense signal in the posterior-inferior portion of the calcaneus, consistent with extensive medullary edema; multilobulated pattern in the plantar portion suggestive of overload injury/bone contusion or stress fracture (0.3 × 0.3 × 3.0 mm, TA 2:38 min).



3 **(3A)** On the left axial rib view, cortical irregularity is seen with an area of slightly hypointense signal on T1 in the lateral portion of a rib (probable fracture site or early callus). **(3B)** Mild signal increase in the subperiosteal/cortical zone on DWI b = 800 s/mm². **(3C)** Signal increase in the cortical/subperiosteal region on DWI b = 1000 s/mm², more pronounced than at b = 800 s/mm². **(3D)** Line of cortical discontinuity in a lateral rib with surrounding high-signal bone and subperiosteal edema. **(3E)** Marked pericortical and medullary hyperintensity in the left lateral rib with subperiosteal edema and high-signal adjacent soft tissue. **(3F)** Linear cortical discontinuity in a right lateral rib with an evident focal linear defect.

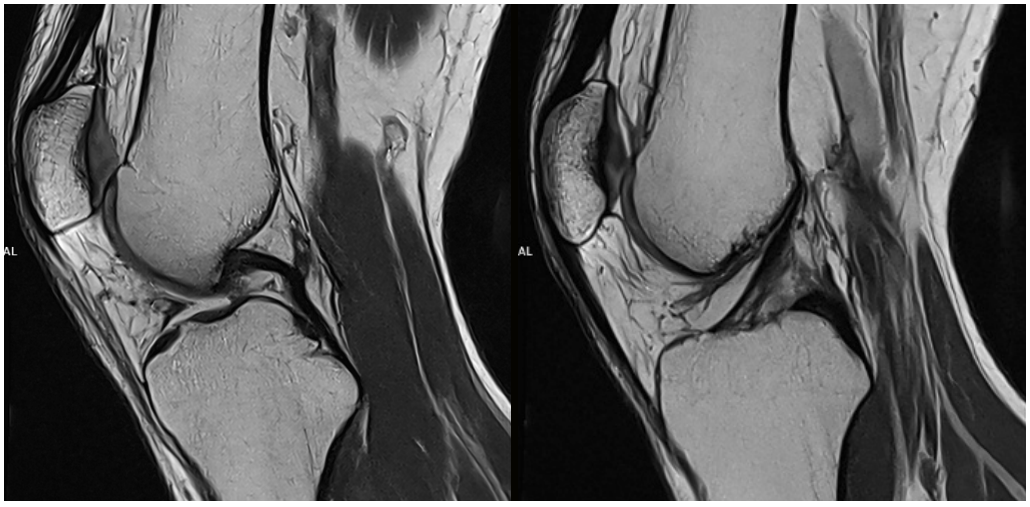


4 **(4A)** Predominantly low-to-intermediate signal intensity in the bone marrow; discrete, patchy areas of increased signal intensity are identified in some phalanges and/or metacarpals, suggestive of mild bone edema or a reactive phenomenon at this level (0.3 × 0.3 × 2.5 mm, TA 3:01 min). **(4B)** Bone marrow with predominantly intermediate signal intensity in the metacarpals and phalanges, without extensive areas of marked hypointensity suggestive of diffuse infiltration (0.2 × 0.2 × 2.5 mm, TA 1:39 min). **(4C)** Significant soft-tissue enlargement along the entire finger, with multiple elongated and nodular hyperintense areas on PD-FS, located in the subcutaneous tissue and along the flexor tendon sheath, with a fluid/edematous appearance, (0.3 × 0.3 × 2.5 mm, TA 1:39 min). **(4D)** Predominantly intermediate-to-high signal intensity in the bone marrow on PD-FS; thickened subcutaneous tissue with multiple rounded/ovoid hyperintense areas on PD-FS, with relatively well-defined borders (0.3 × 0.3 × 2.5 mm, TA 2:29 min).

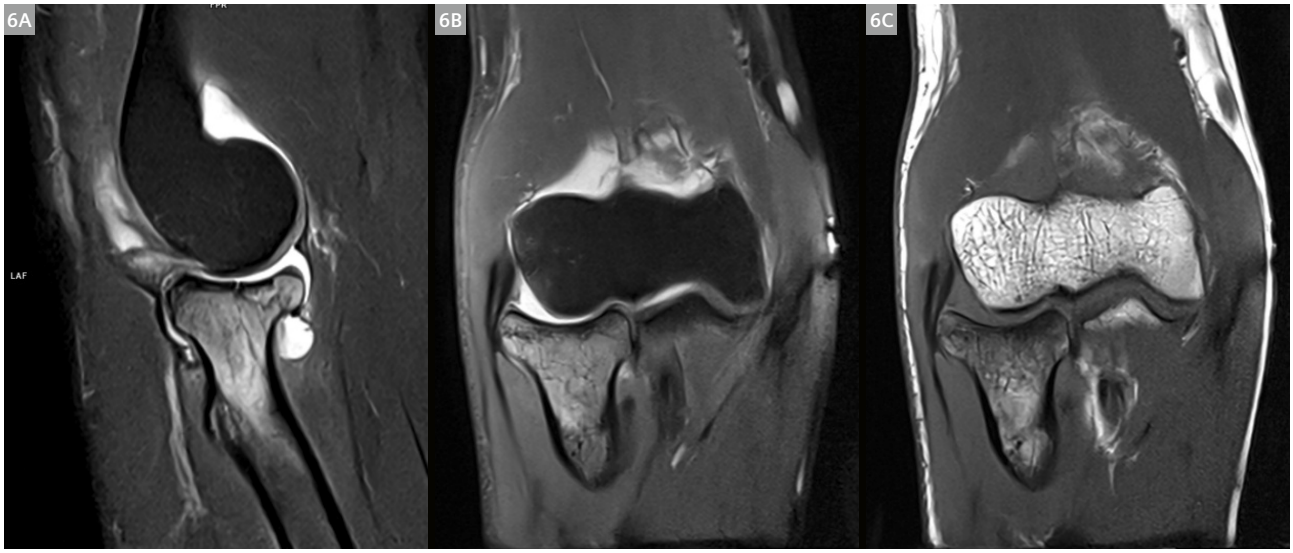
We have observed that 0.55T excels at thoracic studies, imaging near metallic implants[1], pediatric cases, and scenarios that are traditionally limited in routine MRI practice. We can now approach these studies with greater confidence and achieve much better results.

However, AI does not correct acquisitions with incorrect parameters. Rather, it works with the parameters set for each sequence. That is why specific protocols designed by experienced technologists — with application support from Siemens Healthineers — are required.

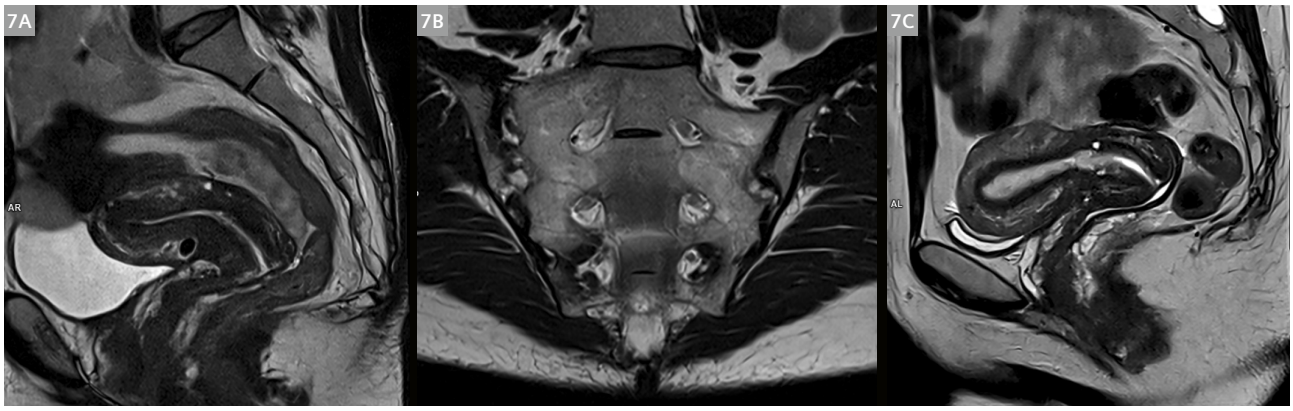
[1] *The MRI restrictions (if any) of the metal implant must be considered prior to patient undergoing MRI exam. MR imaging of patients with metallic implants brings specific risks. However, certain implants are approved by the governing regulatory bodies to be MR conditionally safe. For such implants, the previously mentioned warning may not be applicable. Please contact the implant manufacturer for the specific conditional information. The conditions for MR safety are the responsibility of the implant manufacturer, not of Siemens Healthineers.*



5 Sagittal thin-sliced images to evaluate the cruciate ligaments (0.3 × 0.3 × 2.5 mm, matrix 346 × 384, TA 3:41 min).



6 **(6A)** Articular surfaces with relatively regular contours, without collapse or evident deep chondral defects; bone marrow showing extensive areas of hyperintensity on PD-FS, suggesting marked bone edema within the FOV (0.3 × 0.3 × 3.0 mm, TA 1:20 min). **(6B)** Hyperintense joint fluid is seen in the elbow joint (medial and lateral recesses), consistent with joint effusion and in line with the findings on the sagittal plane (0.3 × 0.3 × 3.0 mm, TA 2:33 min). **(6C)** Bone marrow with heterogeneous fat signal, with hypointense areas in the radius suggesting significant bone contusion on this slice (0.3 × 0.3 × 3.0 mm, TA 1:44 min).



7 **(7A)** T2-weighted sagittal TSE (0.24 × 0.4 × 3.0 mm, matrix 403 × 448, TA 3:00 min).
(7B) Oblique coronal TSE with T2 weighting (0.4 × 0.4 × 3.0 mm, matrix 403 × 448, TA 3:09 min).
(7C) Oblique sagittal view aligned with the uterus; T2-weighted TSE (0.4 × 0.4 × 3.0 mm, matrix 403 × 448, TA 3:09 min).

Implications for healthcare systems

The MAGNETOM Free.Star system can enable greater MRI access and equity. The combination of lower installation costs, reduced energy consumption, and AI-driven capabilities make it possible to provide MRI services in settings where they were previously limited, thereby reducing waiting lists for patients.

Importantly, this is a complementary ecosystem: 0.55T systems do not replace 1.5T or 3T systems. Instead, they complement them within the diagnostic network, optimizing costs and turnaround times.

Conclusion

The 0.55T MAGNETOM Free.Star is a modern reinterpretation of a lower-field MRI system that balances diagnostic quality, artifact reduction, operational efficiency, and accessibility. True clinical value comes from the combination of advanced technology, AI, and human expertise.

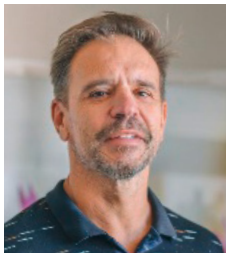
Acknowledgments

Special thanks to Javier Ulloa Salvo and Julián Cuba of the LATAM education team at Siemens Healthineers.

Contact

Lic. Carlos Raúl Sanchez
Department of MRI, Imágenes MDQ
Clínica Colón
Av. Colón 3629
B7600 Mar del Plata, Buenos Aires
Argentina
cerese60@yahoo.com.ar





Claudio Milicchio, M.D.
Department of Diagnostic Imaging,
Imágenes MDQ
Clínica Colón
Av. Colón 3629
B7600 Mar del Plata, Buenos Aires
Argentina
direccion@imagenesmdq.com.ar